TWO-DIMENSIONAL MODELING OF THERMAL GRADIENTS IN THE CORE OF A PRIMARY STANDARD VACUUM GRAPHITE CALORIMETER, IN A SQUARE-FOLDED GEOMETRY*

CRISTINA-ELENA IONIȚĂ and DANIEL RADU

"Al.I. Cuza" University, Faculty of Physics, Carol I Blvd., No.11, 700506, Iasi, Romania
E-mails: cristina_elena_ionita@yahoo.com; dradu@uaic.ro

Received September 5, 2011

The spatio-temporal distribution of temperature change in the core of a vacuum graphite calorimeter (used as a primary standard for therapy-level dose measurements) was determined in the frame of a two-dimensional analytical model for a square-folded geometry. This was done in order to analyze the influence of thermal gradients which appear in the calorimeter's absorber due to the point-like heating by ultra small NTC thermistors (during the electrical calibration of the calorimeter) on the homogeneous heating of the calorimeter core. It was found that after approximately two seconds from the end of the heating period, the temperature change produced by point-like heating of the core is not significantly different (up to 0.1 %) to a uniform heating.

Key words: graphite calorimetry, thermal gradients, dose measurements.

1. INTRODUCTION

As it is known, calorimetry is the basis of almost all absolute measurements of radiation absorbed dose at therapy-level dose rates, usually in graphite or water. It is the most suitable primary standard for radiation absorbed dose because the measurement of temperature rise in a calorimeter comes closer than other methods to providing a direct measurement of the full energy imparted to matter by radiation.

There are three basic modes to operate a graphite calorimeter: quasi-adiabatic, heat-loss-compensated and isothermal modes. The most frequently used calibration method for a primary standard calorimeter which is operated in the quasi-adiabatic mode or in the heat-loss-compensated mode is the comparative method [1, 2]: the response of the calorimeter temperature sensor to an accurately measured heat input is compared with the same response to radiation. This calibration is usually performed by simultaneously dissipating a measured amount of electrical energy in thermistors

* Paper presented at the 12th International Balkan Workshop on Applied Physics, July 6–8, 2011, Constanta, Romania.

that are embedded in both the core (that plays the role of the radiation absorber) and the jacket [3, 4]. Because this calibration method is a comparative one, it becomes very important to ensure that the calorimeter core is identically heated in the two situations: (i) by the irradiation beam and (ii) by the electrical power dissipated in the core through the heating thermistors. Actually, this condition is not exactly satisfied because the core and the components near the core are heated uniformly when the calorimeter is irradiated with beams of rather high-energy – so that, the core thermal gradients are negligible – whereas during an electrical heating the same bodies are non-uniformly heated and consequently thermal gradients unavoidably appear.

There are two major reasons for the appearance of the temperature gradients:

(i) the inhomogeneous electrical heating of the calorimeter bodies and

(ii) the thermal barriers between the thermistors and the material from which the calorimeter bodies (especially the core and the jacket) are made – that is the graphite.

The second factor can be easily managed by ensuring a good thermal contact between the thermistors and the surrounding medium (graphite). For instance, this can be done by mounting the thermistors in their fixed places (see the Fig. 3 from reference [5]) with epoxy resin [6]. Nevertheless, the first factor is more difficult to eliminate. Along the whole history of the graphite calorimetry many researchers proposed different methods in order to reduce as much as possible the effects of this factor. In present, in order to reduce the influences of thermal gradients caused by the inhomogeneous electrical heating of the bodies, an increased number of heating thermistors is used. Of course, these thermistors are spatially distributed according to the symmetry of the bodies [7]. Because the construction of the core (and, in particular, the mounting of the thermistors) is not so easy, it becomes important to know if, from the temperature gradient magnitude point of view, the number of heating thermistors is indeed decisive. Intuitively, on the one hand the magnitude of the temperature gradients decreases with the number of heating thermistors but, on the other hand, an increased number of heating thermistors leads to greater systematic errors. So, it is clear that, to put in accordance these two contradictory situations some compromise is needed. Anyhow, in order to make a valuable analysis that permits to take the best decision and to choose the best solution it's very important also to know as exactly as possible the spatio-temporal distribution of the temperature in the electrically heated bodies of the calorimeter.

In a previous study [8], using the simplest model for the graphite absorber (*i.e.*, the one-dimensional model), the authors have estimated the time after the end of the heating period necessary to thermal gradients to disappear quasi-totally:

$$t_{r,\ \max} = \frac{1}{\beta} \ln\left(\frac{a^2}{0.001 \cdot 3\, k\, t_h} \right) \cong 1{,}6 \text{ s}\,, \qquad (1)$$

the significance of the quantities involved in this formula being given in the next section. The aim of the present study is to evaluate the same time (more precisely defined, it is about the time after the end of the heating period starting since the temperature change produced by pointlike heating of the core during the electrical calibration is not significantly different – up to 0.1 % – to the uniform heating caused by a radiation beam in the calorimeter), but using a more realistic model, namely, a two-dimensional model in a square-folded geometry.

2. THE TWO-DIMENSIONAL MODELING OF THERMAL GRADIENTS

The schematic configurations of the graphite calorimeter and graphite calorimeter core alone analyzed in this paper are graphically represented in Fig. 1 (see the reference [9]) and Fig 2, respectively.

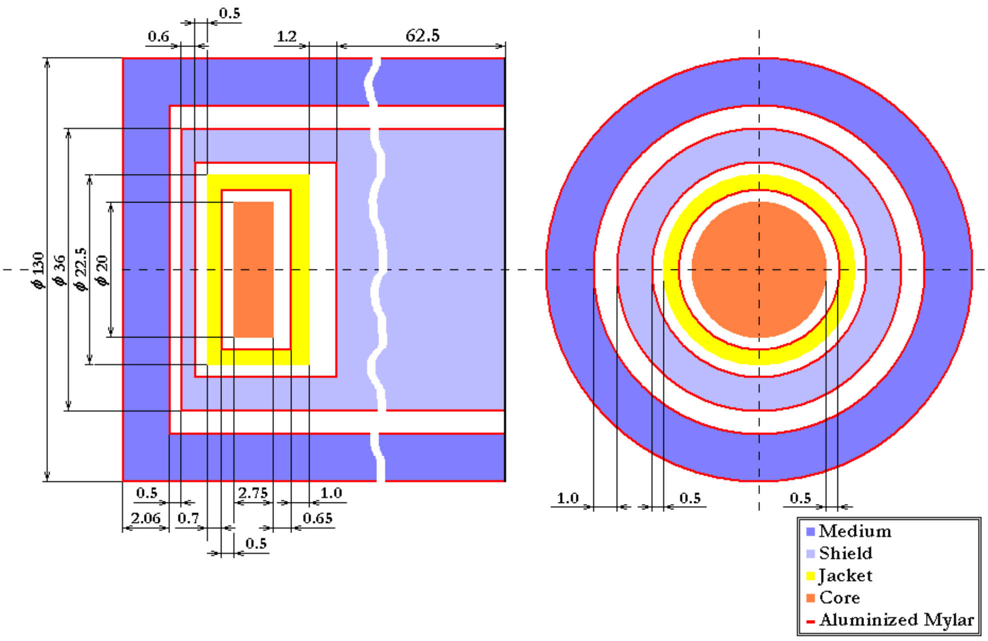

Fig. 1 – The schematic configuration of a graphite calorimeter.

Since the temperature gradients cannot be completely removed by any mean, it's very important, at least, to know the magnitude of these gradients and the weight of their effects on thermal behaviour of a graphite calorimeter. This is the reason why the knowledge of spatio-temporal temperature distribution in the heated bodies of a graphite calorimeter is of a great importance.

In order to find the spatio-temporal distribution of the temperature in the calorimeter core the following second order partial derivative equation must be solved for the scalar field $\phi_{core}(x, y, z, t) \equiv \phi_1$, which represents the temperature change[1] (K) of the core graphite:

$$C_1 V_1^{-1} \frac{\partial \phi_1}{\partial t} - k\left(\frac{\partial^2 \phi_1}{\partial x^2} + \frac{\partial^2 \phi_1}{\partial y^2} + \frac{\partial^2 \phi_1}{\partial z^2}\right) - \mathcal{P}_1(x, y, z, t) = 0, \quad (2)$$

with corresponding initial and boundary conditions.

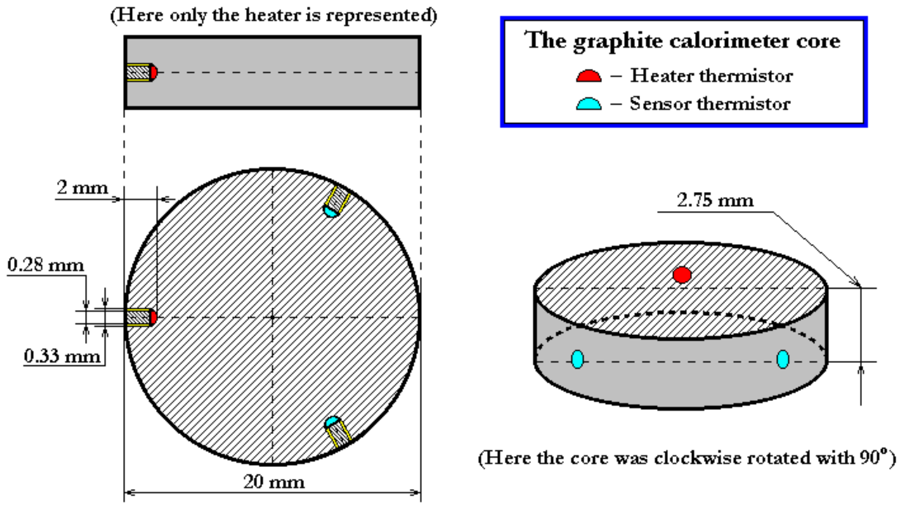

Fig. 2 – The schematic core structure of a graphite calorimeter.

In eq. (2) C_1 is the heat capacity $(\mathrm{J} \times \mathrm{K}^{-1})$ of the core, V_1 is the volume (m^3) of the core, k is the graphite thermal conductivity $(\mathrm{W} \times \mathrm{m}^{-1} \times \mathrm{K}^{-1})$ and $\mathcal{P}_1(x, y, z, t)$ is the spatial density of the electrical power $(\mathrm{W} \times \mathrm{m}^{-3})$ "pumped" in the core. From the mathematical point of view it seems – for the moment – to be enough to solve the problem given by equation (2), taking also into account the corresponding initial and boundary conditions. However, when the limit conditions are taken into account the real problem becomes more complicated, because these

[1] The "temperature change" of any calorimeter body represents the temperature rise (K or °C) of the corresponding body, above the constant temperature of the surrounding medium: $\phi_i = \phi_i^{body} - \phi_m = \phi_i^{body} - 298.15\ K$, where ϕ_i^{body} is the absolute temperature (K) of the "i"-body, and the subscript index $i = 1,\ 2,\ 3$ refers to the core, jacket and shield, respectively.

conditions directly depend on the scalar time-dependent field representing the temperature change (K) of the jacket, $\phi_2 = \phi_2(x, y, z, t)$. The corresponding mathematical problem, referring to the jacket, has limit conditions that on their turn depend on the scalar field representing the temperature change (K) of the shield, $\phi_3 = \phi_3(x, y, z, t)$; moreover, they also depend on certain additional quantities as for example: the heat transfer coefficients between the calorimeter bodies, the emissivities of the bodies' surfaces, the geometrical factors of the bodies in the calorimeter etc. Obviously, the two new scalar fields, $\phi_2 = \phi_2(x, y, z, t)$ and $\phi_3 = \phi_3(x, y, z, t)$ represent two unknown quantities for the problem given by the equation (2), with the corresponding limit conditions, which thus proves to be insufficient to give a complete and unique solution to the problem (the number of unknown quantities is greater than the number of equations).

In fact, to exactly solve – even numerically – the problem of spatio-temporal distribution of temperature in the core of a graphite calorimeter is a task not easy at all. As results from the above considerations regarding the boundary conditions for equation (2), the solution of this problem is tightly related to the solutions corresponding to the jacket and shield. Thus, to be precise, the real mathematical problem that must be solved in order to find the complete thermal behaviour of the whole three-body graphite calorimeter – and implicitly the solution of the problem that corresponds only to the core – is the following:

$$\begin{cases} C_1 V_1^{-1} \dfrac{\partial \phi_1}{\partial t} - k\left(\dfrac{\partial^2 \phi_1}{\partial x^2} + \dfrac{\partial^2 \phi_1}{\partial y^2} + \dfrac{\partial^2 \phi_1}{\partial z^2}\right) - \mathcal{P}_1(x, y, z, t) = 0, \\ C_2 V_2^{-1} \dfrac{\partial \phi_2}{\partial t} - k\left(\dfrac{\partial^2 \phi_2}{\partial x^2} + \dfrac{\partial^2 \phi_2}{\partial y^2} + \dfrac{\partial^2 \phi_2}{\partial z^2}\right) - \mathcal{P}_2(x, y, z, t) = 0, \\ C_3 V_3^{-1} \dfrac{\partial \phi_3}{\partial t} - k\left(\dfrac{\partial^2 \phi_3}{\partial x^2} + \dfrac{\partial^2 \phi_3}{\partial y^2} + \dfrac{\partial^2 \phi_3}{\partial z^2}\right) - \mathcal{P}_3(x, y, z, t) = 0, \end{cases} \quad (3)$$

with enough complicated limit conditions that are not given here.

Because of the great difficulty in finding the exact real solution of this problem, in the following we shall restrict only to the problem given by equation (2) and relating new limit conditions, considering – in the first approximation – that the jacket and shield have only constant and isotropic influence on the thermal state of the core. So, for the moment, this problem will be solved supposing that $\phi_2(x, y, z, t) = \phi_{02} = const.$ and $\phi_3(x, y, z, t) = \phi_{03} = const.$ In this way, the only difficulty in finding an analytical solution for this new problem can be brought by the third term in equation (2), which could introduce some difficulties related only to the exact geometry of the heating thermistor. If, for example, the thermistor dimensions are neglected with respect to those of the whole core (*i.e.*, if an idealized point-like thermistor is considered), then equation (2) becomes

$$C_1 V_1^{-1} \frac{\partial \phi_1}{\partial t} - k\,\Delta\phi_1 = P_1\,\delta(x - x_0)\,\delta(y - y_0)\,\delta(z - z_0), \tag{4}$$

where P_1 is the constant electrical power (W) applied to the core at the moment $t_0 = 0$, $\delta(x - x_0)$ is the one-dimensional Dirac's "delta" distribution and $P_0(x_0, y_0, z_0) = P_0(0,0,h)$ is the location of the point-like thermistor (see the Fig. 3).

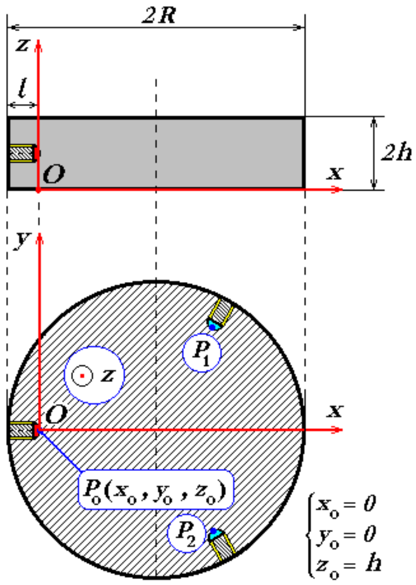

Fig. 3 – The spatial orientation of the Cartesian coordinates.

Without any doubt, excluding the exact analytical solution, the most precise and reliable approach of the problem of magnitude and influence of the thermal gradients appearing in the core of a real graphite calorimeter during an electrical calibration run is that based on a three-dimensional model within the frame of finite element numerical method. However, this kind of approach is quite complicated and time consuming; besides, if the real configuration of a graphite calorimeter is intended to be analyzed, a huge computing-power is usually required. Despite of this, the analytical study of a two-dimensional model proves to be very helpful because – as it will be seen at the end – the results obtained in this model are so close to those previously obtained in the analytical study of one-dimensional model, that lead us to the conclusion that the main quantity involved in the model – the relaxation time t_r – would be approximately the same for a thin three-dimensional object, like is the core of a graphite calorimeter; the relaxation time is the time needed to reduce the maximum of $\phi(x,\ t)$ to the final temperature change in the core, ϕ_{∞}. Actually, the real calorimeter core is a disc (roughly of diameter 20.00 mm and thickness 2.75 mm – see the Fig. 2); although the shape is different to the square modelled in this paper, a similar estimate of the relaxation time t_r would be expected from this shape too.

To find the analytical solution of equation (4) even proves to be difficult and because of this in the following this equation will be solved only in two-dimensional case.

The simpler one-dimensional case was analyzed in detail in a previous work [8]. By solving the one-dimensional diffusion equation for temperature change $\phi(x,\ t)$, the authors found that the relaxation time, t_r, has the value $t_r = 1.3687$ s. Using the equality

$$-\frac{1}{12}+\frac{1}{4}\xi^{2}=\sum_{n=1}^{\infty}\frac{(-1)^{n}}{n^{2}\pi^{2}}\cos\left(n\pi\xi\right), \tag{5}$$

the analytical solution of the one-dimensional problem

$$\frac{\partial\phi(x,t)}{\partial t}=\alpha\frac{\partial^{2}\phi(x,t)}{\partial x^{2}}$$

(where α is the graphite thermal diffusivity) with the initial and boundary conditions

$$\phi(x,0)=0,\ \ \phi(x,\infty)=\phi_{\infty},\ \ \left.\frac{\partial\phi}{\partial x}\right|_{x=0}=0,\ \ \left.\frac{\partial\phi}{\partial x}\right|_{\substack{x=a\\ t\le t_h}}=J_0=\text{const.},\ \ \left.\frac{\partial\phi}{\partial x}\right|_{\substack{x=a\\ t>t_h}}=0, \tag{6}$$

was found by means of Fourier method; it is given by

$$\phi(x,t)=\frac{\phi_{\infty}}{t_h}\times$$
$$\left\{t-\left(t-t_h\right)\theta(t-t_h)+2\sum_{n=1}^{\infty}\left[\left(1-e^{-\beta n^{2}t}\right)-\left(1-e^{-\beta n^{2}(t-t_h)}\right)\theta(t-t_h)\right]\frac{(-1)^{n}}{\beta n^{2}}\cos\frac{n\pi x}{a}\right\}, \tag{7}$$

where

$$\theta(y)=\begin{cases}0, & y<0,\\ 1, & y\ge 0\end{cases} \tag{8}$$

is the Heaviside function (the step function) and β is defined by $\beta a^{2}=k\pi^{2}$, k being the graphite thermal conductivity.

The values for key quantities used in [8] are the following: the linear dimension of the core was $a = 20$ mm, the heating time was $t_h = 60$ s and the final temperature change was $\phi_\infty = 1$ mK. The relaxation time was obtained considering the time (after t_h) needed to get to 0.1 % of the final ϕ_∞ value. A maximum value for t_r ($t_{r,\,max}$), relating to the experimental situation when heating is off was also evaluated, giving a theoretical value of $t_{r,\,max} \cong 1.6$ s.

Let's now focus our attention on the two-dimensional problem. As the temperature change ϕ in an electrical calibration is dominated by the heat conduction, it can be calculated by solving the well known heat equation [10]:

$$\frac{\partial \phi}{\partial t} = \alpha\ \Delta\phi ,$$

where the diffusivity α is given by $\alpha = k/\rho c$ (k is the thermal conductivity, ρ is the mass density and c is the specific heat capacity of the material (graphite)).

Let suppose that the core is thermally isolated and starts at a uniform temperature. Thus, when the core is electrically heated the temperature gradient at the heater (the thermistor) is proportional to the rate of heating applied. Of course, initially the region nearest the thermistor increases in temperature faster than the rest of the core.

Table 1

The values of the main quantities involved in the model

Quantity	Symbol	Value
Graphite density	ρ	$1790\ \text{kg} \times \text{m}^{-3}$
Thermal diffusivity of graphite at 25°C	α	$8.271 \times 10^{-5} \text{m}^2 \times \text{s}^{-1}$
Graphite thermal conductivity at 25°C	k	$106.537\ \text{W} \times \text{m}^{-1} \times \text{K}^{-1}$
Specific heat capacity of graphite at 25°C	c	$719{,}59\ J \times \text{kg}^{-1} \times \text{K}^{-1}$
Core diameter	d	$2.0 \times 10^{-2}\text{m}$
Core height	h	$2.75 \times 10^{-3}\text{m}$
Core heating time	t_h	60 s
Heating energy input	Q	$1112.82 \times 10^{-6}\text{J}$

If the heating continues for long enough (more precisely, if the heating continues for long times after the complete disappearance of thermal gradients), then practically the whole core will increase in temperature at the same rate. When the heating is switched off the temperature gradient at the heater is zero, but there will still be a gradient throughout the rest of the core. After the heating has been off for some time, the gradient in the core dies away to zero and the core temperature is again practically uniform throughout. The final temperature change in the core can be calculated from the energy conservation law and it is $\phi_\infty = Q/mc$, where Q is the heating energy input and m is the core mass. Obviously, it is simpler to express the power input in terms of ϕ_∞ than the temperature gradient at the heater.

The two-dimensional form of the heat equation is

$$\frac{\partial\phi(x, y,\ t)}{\partial t} = \alpha\left(\frac{\partial^2\phi(x, y,\ t)}{\partial x^2} + \frac{\partial^2\phi(x, y,\ t)}{\partial y^2}\right). \tag{9}$$

The initial and boundary conditions for this equation that model the situation similar to an adiabatic electrical calibration are as follows:

(i) initially the temperature starts uniform;

(ii) the boundary of the square is insulated, except along a small section 2ε near the centre of one side where there is a constant rate of heat input for a time interval t_h;

(iii) the final temperature is ϕ_∞.

From the mathematical point of view, the question turns to solve the following problem: Let's find the spatio-temporal distribution of temperature, $\phi = \phi(x, y, t)$, within an isotropic, homogeneous and thermo-conducting material of mass m and specific heat capacity c, that is distributed on a squared surface $\{x, y\} \in [0,\ a] \times [0,\ a]$, knowing that in the regions $x < 0,\ y < 0,\ y > a$ and $x > a$ (except along a small section 2ε near the centre of this side) there is an infinite perfect thermo-insulating material, whereas along that section of length 2ε it is applied a constant heating flux (there is a constant rate of heat input) during the time interval $t \in [0,\ t_h]$, so that the total heat input is Q. The material starts at a uniform temperature, *i.e.* $\phi(x, y, 0) = 0$.

If the heat equation (9) is re-written in a form analogous to that given by equation (4), *i.e.*, with a source term,

$$\hat{D}\phi(x, y, t) = \frac{1}{2\varepsilon} J_0\ \chi(y, t, \varepsilon), \tag{10}$$

where the operator $\hat{D}$ is given by

$$\hat{D} \equiv \frac{\partial}{\partial t} - \alpha\ \Delta_2 = \frac{\partial}{\partial t} - \alpha\ \left(\frac{\partial^2}{\partial x^2} + \frac{\partial^2}{\partial y^2}\right), \tag{11}$$

J_0 is a constant having the dimensions of a heating flux and $\chi(y, \varepsilon)$ is a special function (a distribution, in fact), given by

$$\chi(y, t, \varepsilon) = C\left[1 - \theta(t - t_h)\right]\left[\theta\left(y - \frac{a}{2} + \varepsilon\right) + \theta\left(\frac{a}{2} + \varepsilon - y\right) - 1\right], \tag{12}$$

then the problem can be solved with the aid of the formalism offered by the functional analysis and distributions theory [10]. In formula (12) C is a pure constant having the dimension $\mathrm{m}^2 \times \mathrm{s}^{-1}$, while $\theta(\xi)$ is the step (Heaviside) function defined by (8).

The boundary conditions for equation (10) are graphically represented in Fig. 4 and mathematically can be expressed – including the initial and "final" conditions – as follows

$$\begin{cases} \phi(x,y,0)=0, \quad (\forall)\ x\in[0,a], y\in[0,a], \\ \phi(x,y,\infty)=\phi_{\infty}, \quad (\forall)\ x\in[0,a], y\in[0,a], \\ \left.\dfrac{\partial\phi}{\partial x}\right|_{x=0}=0,\ (\forall)\ y\in[0,a],\ t\in[0,\infty), \\ \left.\dfrac{\partial\phi}{\partial x}\right|_{x=a}=J_0\left[1-\theta(t-t_h)\right]\left[\theta\left(y-\dfrac{a}{2}+\varepsilon\right)+\theta\left(\dfrac{a}{2}+\varepsilon-y\right)-1\right], \\ \qquad (\forall)\ y\in[0,a],\ t\in[0,\infty), \\ \left.\dfrac{\partial\phi}{\partial y}\right|_{y=0}=0,\ (\forall)\ x\in[0,a],\ t\in[0,\infty), \\ \left.\dfrac{\partial\phi}{\partial y}\right|_{y=a}=0,\ (\forall)\ x\in[0,a],\ t\in[0,\infty). \end{cases} \tag{13}$$

Using the Fourier method, the problem leads to a Helmholtz-type equation for the spatial part of the solution, $Z_{\lambda}(x,y)$, the subscript index λ representing the eigenvalues of the mixed operator $\hat{D}$ (the corresponding eigenvalue problem being given by the following equation: $\hat{D}\Psi_{\lambda}=\lambda\,\Psi_{\lambda}\left[=\lambda\,T(t)Z_{\lambda}(x,y)\right]$).

Making use of the fact that on the square $S_a=\left\{(x,y)\middle|\ 0\le x\le a,\ 0\le y\le a\right\}$ the orthonormal modes are given by

$$U_{nm}(x,y)=\frac{2}{a}\sin\frac{n\pi}{a}x\ \sin\frac{m\pi}{a}y,$$

$$V_{nm}(x,y)=\frac{2}{a}\cos\frac{n\pi}{a}x\ \cos\frac{m\pi}{a}y,$$

and the step (Heaviside) function $\theta(\xi)$ and delta (Dirac) function $\delta(\xi)$ satisfy the functional relations

$$\int \delta(\xi)\,\mathrm{d}\xi = \theta(\xi); \quad \int \theta(\xi)\,\mathrm{d}\xi = \xi\,\theta(\xi); \quad \mathrm{d}\theta(\xi) = \delta(\xi)\,\mathrm{d}\xi\,,$$

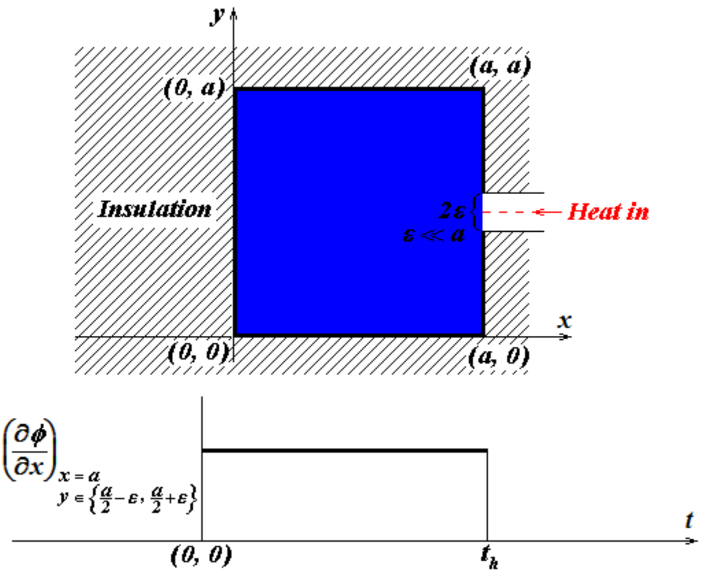

Fig. 4 – Two-dimensional boundary conditions.

the final solution of equation (10) – or equivalently – (9) is writes as follows

$$\begin{aligned}\phi(x,y,t) = \frac{\phi_\infty}{t_h}\Bigg\{ & t-(t-t_h)\theta(t-t_h) + 2\sum_{n=1}^{\infty}\Big[\left(1-\mathrm{e}^{-\beta n^2 t}\right)-\left(1-\mathrm{e}^{-\beta n^2 (t-t_h)}\right)\times \\ & \theta(t-t_h)\Big]\frac{(-1)^n}{\beta n^2}\cos\frac{n\pi x}{a} + 2\sum_{m=1}^{\infty}\Big[\Big(\Big[\left(1-\mathrm{e}^{-\beta m^2 t}\right)-\left(1-\mathrm{e}^{-\beta m^2 (t-t_h)}\right)\theta(t-t_h)\Big]\times \\ & \frac{1}{\beta m^2} + 2\sum_{r=1}^{\infty}\frac{(-1)^r}{\beta\left(m^2+r^2\right)}\cos\frac{r\pi x}{a}\Big[\left(1-\mathrm{e}^{-\beta\left(m^2+r^2\right)t}\right)-\left(1-\mathrm{e}^{-\beta\left(m^2+r^2\right)(t-t_h)}\right)\times \\ & \theta(t-t_h)\Big]\Big)\cos\frac{m\pi}{2}\cos\frac{m\pi y}{a}\Big]\Bigg\}\end{aligned} \tag{14}$$

and gives the two-dimensional spatio-temporal distribution of temperature change in the core (modelled by a square-shaped bi-dimensional object) of the graphite calorimeter.

3. RESULTS AND DISCUSSION

The dependence of temperature change ϕ on its spatial variables (x and y) for two relevant values of temporal variable t ($t = 0.005\ t_h$ and $t = 1.1\ t_h$) is graphically represented in Figs. 5 and 6.

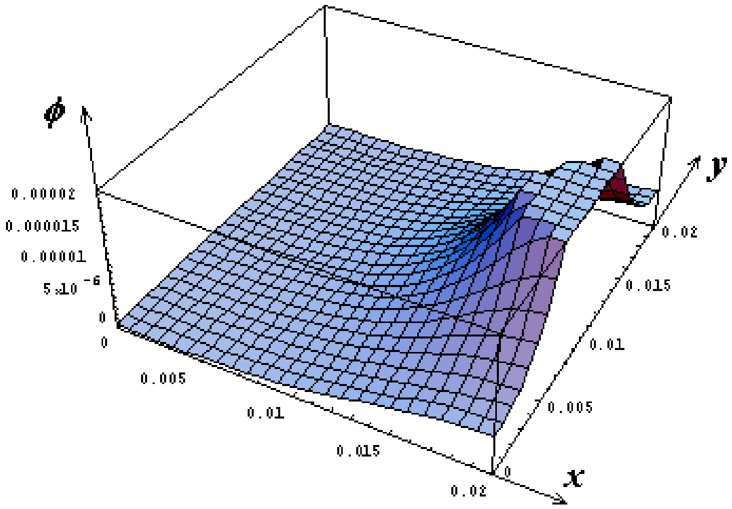

Fig. 5 – The spatial dependence of $\phi = \phi(x, y, t = 0.005\ t_h)$.

As Fig. 5 shows, at the very beginning of the heating process the temperature change has significant values only around the small region through which the heat flux enters into the core, *i.e.*, the small $y-$interval centered on $y = a/2$, located at $x = a$ and having the length 2ε $(\varepsilon \ll a)$ – see the boundary conditions (13) that are graphically illustrated in Fig. 4.

Between the instants $t = 0.5\ t_h$ and $t = t_h$ the changes in the shape of spatio-temporal distribution of temperature $\phi(x, y, t)$ are very small (practically, they are unobservable). At the instant $t = 1.1\ t_h$ the variation of $\phi(x, y, t)$ with the spatial coordinate y has already disappeared, while the x-variation of $\phi(x, y, t)$ is quite small (in Fig. 6, on the "vertical" ϕ-axis the three numerical values are equal).

At the instant $t = 1.5\ t_h$ the temperature field is already uniform, which means that the temperature gradient have completely disappeared.

Let's t_r be the time taken for the maximum of $\phi(a, a/2, t)$ – which corresponds to the point of maximum/fastest variation of temperature change – to reduce to $0.1\ \%$ of ϕ_∞.

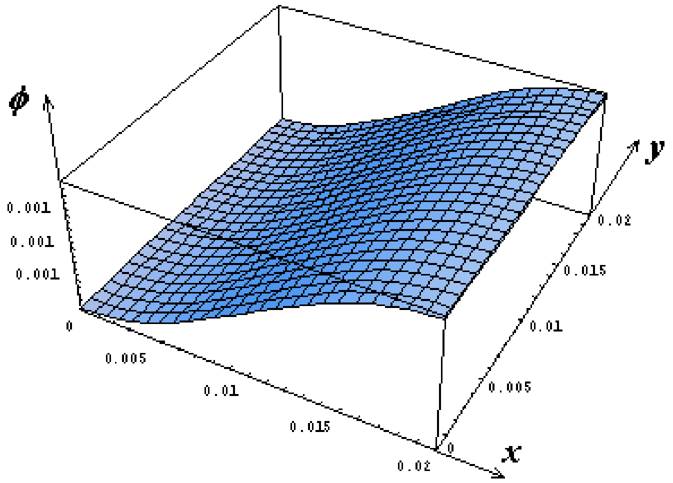

Fig. 6 – The spatial dependence of $\phi = \phi\left(x, y, t = 1.1\ t_h\right)$.

With the physical properties identical to those of the calorimeter core, for length a of 20 mm, a heating time t_h of 60 s and a final temperature change ϕ_∞ of 1 mK, the expression (2.13) was numerically evaluated using the *Mathematica 5.0* software; it was found that the time t_r (after t_h) to get to 0.1 % of ϕ_∞ is $\left(t_r\right)_{0.1\ \%} = 1.368738$ s (see the Fig. 7).

If $1 << \beta t < \beta t_h$ (in our case $\beta \cong 2.041\ \mathrm{s}^{-1}$) then the whole of the core will increase in temperature approximately at the same rate, $\phi(x, y, t)$ reaches a quasi-constant shape in spatial variables x and y and rises quasi-linearly in temporal variable t.

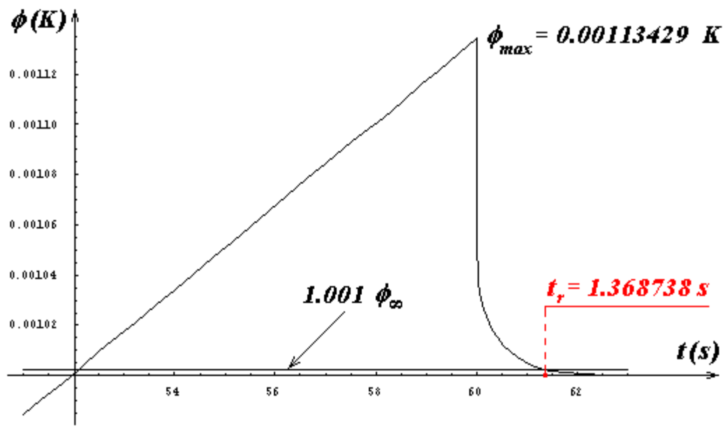

Fig. 7 – The time dependence of temperature rise $\phi\left(x, y, t\right)$ at the point $x = a$, $y = a/2$.

Indeed, if $1 << \beta t$, then $e^{-\beta n^2 t} \approx 0,\ e^{-\beta m^2 t} \approx 0,\ e^{-\beta\left(m^2+r^2\right)t} \approx 0$, and (14) becomes

$$\phi(x,y,t) \cong \frac{\phi_\infty}{\beta t_h}\left(\text{PolyLog}\left[2,-\mathrm{e}^{-\frac{i\pi x}{a}}\right]+\text{PolyLog}\left[2,-\mathrm{e}^{\frac{i\pi x}{a}}\right]\right)+\frac{\phi_\infty}{2\beta t_h}\times$$
$$\left(\text{PolyLog}\left[2,\mathrm{e}^{i\left(\frac{\pi}{2}-\frac{\pi y}{a}\right)}\right]+\text{PolyLog}\left[2,\ \mathrm{e}^{\mathrm{i}\left(\frac{\pi}{2}+\frac{\pi y}{a}\right)}\right]+\text{PolyLog}\left[2,\ -\mathrm{e}^{\mathrm{i}\pi-i\left(\frac{\pi}{2}-\frac{\pi y}{a}\right)}\right]+\right.$$
$$\left.\text{PolyLog}\left[2,\ -\mathrm{e}^{i\pi-i\left(\frac{\pi}{2}+\frac{\pi y}{a}\right)}\right]\right)+\frac{4\phi_\infty}{\beta t_h}\sum_{n=1}^{\infty}\frac{\cos\frac{n\pi}{2}\cos\frac{n\pi y}{a}}{4n\left(1+n^2\right)}\ \mathrm{e}^{\frac{\mathrm{i}\pi x}{a}}\left(i\ \text{Hypergeometric2F1}\left[1,\right.\right.$$
$$\left.1-in,2-in,-\mathrm{e}^{-\frac{i\pi x}{a}}\right]-n\ \text{Hypergeometric2F1}\left[1,1-in,2-in,-e^{-\frac{\mathrm{i}\pi x}{a}}\right]+i\ e^{\frac{2i\pi x}{a}}\times$$
$$\text{Hypergeometric2F1}\left[1,1-in,2-in,-\mathrm{e}^{\frac{\mathrm{i}\pi x}{a}}\right]-\mathrm{e}^{\frac{2i\pi x}{a}}n\ \text{Hypergeometric2F1}\left[1,1-in,2-\right.$$
$$\left.\mathrm{i}n,-e^{\frac{i\pi x}{a}}\right]-i\ \text{Hypergeometric2F1}\left[1,1+in,2+in,-e^{-\frac{i\pi x}{a}}\right]-n\ \text{Hypergeometric2F1}\left[1,\right.$$
$$\left.1+\mathrm{i}n,2+\mathrm{i}n,-\mathrm{e}^{-\frac{\mathrm{i}\pi x}{a}}\right]-\mathrm{i}\ \mathrm{e}^{\frac{2\mathrm{i}\pi x}{a}}\ \text{Hypergeometric2F1}\left[1,1+\mathrm{i}n,2+\mathrm{i}n,-\mathrm{e}^{\frac{\mathrm{i}\pi x}{a}}\right]-\mathrm{e}^{\frac{2\mathrm{i}\pi x}{a}}n\times$$
$$\left.\text{Hypergeometric2F1}\left[1,1+\mathrm{i}n,2+\mathrm{i}n,-\mathrm{e}^{\frac{\mathrm{i}\pi x}{a}}\right]\right),$$

where $\text{PolyLog}[n,\ z]$ gives the polylogarithm function: $\mathrm{Li}_n(z)=\sum_{k=1}^{\infty}\frac{z^k}{k^n}$, while the special function denoted by $\text{Hypergeometric2F1}[a,b;c;z]$ is a special case of $\text{HypergeometricPFQ}\left[\left\{a_1,\cdots,a_p\right\};\left\{b_1,\cdots,b_q\right\};z\right]$ – the generalized hypergeometric function ${}_pF_q\left(\vec{a};\vec{b};z\right)$, which has the following series expansion: ${}_pF_q\left(\vec{a};\vec{b};z\right)=\sum_{k=0}^{\infty}\frac{\left(a_1\right)_k\left(a_2\right)_k\cdots\left(a_p\right)_k}{\left(b_1\right)_k\left(b_2\right)_k\cdots\left(b_p\right)_k}\frac{z^k}{k!}$. Of course, ${}_2F_1\left(a,b;c;z\right)=\sum_{k=0}^{\infty}\frac{(a)_k(b)_k}{(c)_k}\frac{z^k}{k!}$. Using the mathematical special properties of polylogarithm and hypergeometric functions, the above expression for $\phi(x,y,t)$, in the approximation $1<<\beta t<\beta t_h$, writes

$$\phi(x,y,t)=\frac{\phi_\infty}{t_h}t+\frac{\pi^2\phi_\infty}{2\beta t_h}\left(\frac{x^2+y^2}{a^2}-\frac{5}{12}\right)+\frac{4\phi_\infty}{\beta t_h}\times$$
$$\sum_{n=1}^{\infty}\left\{\left[A_n+B_n\frac{y^2}{a^2}+\mathcal{O}\left(y^4\right)\right]+\left[C_n+D_n\frac{y^2}{a^2}+\mathcal{O}\left(y^4\right)\right]\frac{x^2}{a^2}+\mathcal{O}\left(x^4\right)\right\}+$$
$$+\mathcal{O}\left(x^4\right)+\mathcal{O}\left(y^4\right),$$

where A_n, B_n, C_n and D_n are simple functions of n, $\cos\frac{n\pi}{2}$, $\sinh\frac{n\pi}{2}$ and $\cosh\frac{n\pi}{2}$. For instance, $A_n=\frac{\pi}{n\,\sinh(n\pi)}\cos\frac{n\pi}{2}$.

In this approximation, the maximum temperature change $\phi_{\max}$ can be obtained from the above relation for $t=t_h$, $x=a$ and $y=a/2$. The result is very close to the maximum value of $\phi(x,y,t)$ evaluated directly from (14), *i.e.*, $\phi_{\max}\cong 1.1343\,\phi_\infty$.

If this state is reached when the heating is turned off (*i.e.* $1<<\beta t_h$), an upper bound on the "relaxation" time $t_{r,\max}$ can be calculated by looking at slowest decay in the Fourier expansion. The time after the heating to get to, for instance, $0.1\ \%$ of ϕ_∞ is less than two seconds.

4. CONCLUSIONS

As it was already mentioned in the first section of the paper, the point-like heating of the core of a graphite calorimeter unavoidably leads to a non-uniform temperature distribution in the core, *i.e.*, to temperature gradients. Of course, the larger the gradients the larger the difference between the two temperature distribution in the core are (that corresponding to an irradiation run and that corresponding to an electrical calibration run). It was shown that the temperature distribution in the core (which is supposed to be a square – two-dimensional model) is non-uniform and the temperature gradients play an important role. Indeed, the calculations show that in the approximation $1<<\beta t$ the maximum temperature change $\phi_{\max}$ is $13.4\ \%$ greater than ϕ_∞ and the time after the heating to get to, for instance, $0.1\ \%$ of ϕ_∞ is $\left(t_r\right)_{0.1\ \%}\cong 1.37\ \text{s}$, while $t_{r,\max}<2\ \text{s}$.

As the relaxation times found from one- and two-dimensional analyses are almost the same, this could suggest that the relaxation time t_r for a thin three-dimensional object would be approximately the same.

Because $(t_r)_{0.1\ \%}$ is an approximate value, it can be certainly stated that the temperature change produced by point-like heating of the core during the electrical calibration is not significantly different (to $0.1\ \%$) to a uniform heating in the calorimeter after approximately two seconds from the end of the heating period. Thus, the thermal gradients can play a significant role only during the first two seconds after the heating period, at all other times the two temperature distributions (corresponding to the irradiation and electrical calibration runs) being quasi the same.

Acknowledgements. This work was supported by the European Social Fund in Romania, under the responsibility of the Managing Authority for the Operational Programme Sector for Human Resources Development 2007-2013 [grant POSDRU/CPP 107/DMI 1.5/S/78342].

REFERENCES

1. S.R. Domen and P.J. Lamperti, *A Heat-Loss-Compensated Calorimeter: Theory, Design and Performance*, Journal of Research of the NBS – A. Physics and Chemistry, Vol. **78A**, No. 5, p. 596, 1974.
2. S.R. Domen, *Advances in Calorimetry for Radiation Dosimetry*, edited by Kenneth R. Kase, Bengt E. Bjarngard and Frank H. Attix, *The Dosimetry of Ionizing Radiation*, Vol. II, Academic Press, Inc., Harcourt Brace Jovanovich, Orlando, San Diego, New-York, Austin, p. 258, 1987.
3. M. Sapoff and R.M. Oppenheim, *Theory and Application of Self-Heated Thermistors*, Proceedings of the IEEE, pp. 1292–1305, 1963.
4. VECO Technical Bulletin MTD131 – *Thermistor Terminology*, VECO Technical Bulletin MCT181 – *Techniques for Testing Thermistors*, VECO Technical Bulletin VM2056 – *Thinistors – Thin Film Thermistors*, VECO Technical Bulletin V1142A – *Reliability of VECO Thermistors*, VECO Product Bulletin MB012, Victory Engineering Corporation, P.O. Box 559, Victory Road, Springfield, New Jersey 07081, TWX: 710-983-4430, 1964.
5. D. Radu, A.S. Guerra, C.E. Ioniță and I. Aştefanoaei, *Heat loss through the connecting thermistor wires in a 3-body graphite calorimeter*, Metrologia, Vol. **47**, Issue 3, pp. 179–191, 2010.
6. J.S. Laughlin and S. Genna, *Calorimetry*, edited by Frank H. Attix and William C. Roesch, *Radiation Dosimetry*, second edition, Vol. II, Academic Press, New-York, San Francisco, London, 1966.
7. J. Daures and A. Ostrowsky, *New constant-temperature operating mode for graphite calorimeter at LNE-LNHB*, Phys. Med. Biol., Vol. **50**, pp. 4035–4052, 2005.
8. C.E. Ioniță, D. Mihailescu and D. Radu, *One dimensional modeling of thermal gradients in the core of a primary standard calorimeter for absorbed dose measurements*, Analele Ştiinţifice ale Universităţii "Al.I. Cuza" Iaşi, Secţiunea "Biomaterials in Biophysics, Medical Physics and Ecology", ISSN 2066 – 3927, Tomul II, pp. 6–20, 2009.
9. C.E. Ioniță, D. Radu and I. Aştefănoaei, *Radiative heat loss correction for 3-body graphite calorimeters*, Acta Physica Polonica, Vol. **118**, No. 4, pp. 333–345, 2010.
10. V.S. Vladimirov, *Ecuaţiile fizicii matematice*, Editura Ştiinţifică şi Enciclopedică, Bucureşti (traducerea celei de-a treia ediţii a cărţii din limba rusă), 1980.